Polym. Korea, Vol. 49, No. 5, pp. 548-555 (2025)
https://doi.org/10.7317/pk.2025.49.5.548
ISSN 2234-8077(Online)

# 유리섬유 강화 PET 복합재에서 Boehmite와 Aluminum Diethylphosphinate의 난연 시너지 효과: 열안정성, 기계적 성능 및 화재 안전성 향상

Xiang Li†, Guirong Xie, and Wenhao Liu
Hunan Chemical Vocational Technology College
(2024년 12월 23일 접수, 2025년 3월 31일 수정, 2025년 4월 15일 채택)

# Synergistic Flame-Retardant Effects of Boehmite and Aluminum Diethylphosphinate in Glass Fiber-Reinforced PET Composites: Enhanced Thermal Stability, Mechanical Performance, and Fire Safety

**Xiang Li†, Guirong Xie, and Wenhao Liu**
*Hunan Chemical Vocational Technology College, Zhuzhou 412000, China*
(Received December 23, 2024; Revised March 31, 2025; Accepted April 15, 2025)

**Abstract:** The properties of glass fiber-reinforced polyethylene terephthalate (GF-PET) composites were investigated using limit oxygen index (LOI) measurement, vertical burning test, cone calorimeter test, thermogravimetric analysis, mechanical properties testing, and hot deformation temperature (HDT) testing. The results showed that appropriate amounts of boehmite (BM) and aluminum diethylphosphinate (ADP) in GF-PET had synergistic flame-retardant effects, and an appropriate amount of BM could improve the hot deformation temperature, mechanical properties, and thermal properties of the ADP/GF-PET composite. When 4% ADP was replaced by 4% BM, the 4-BM/ADP/GF-PET composite achieved a UL-94 V0 rating (2.0 mm) with an LOI of 31 vol%, and the peak of heat release rate (PHRR), average effective heat of combustion (AEHC), total heat rate (THR), and total smoke release (TSR) decreased by 13.9%, 16.7%, 18.8%, and 19.7%, respectively, while the time to ignition (TTI) and fire performance index (FPI) increased by 14.9% and 23.5%, respectively, compared with the ADP/GF-PET composite.

**Keywords:** boehmite, aluminum diethylphosphinate, synergistic flame-retardant effects, glass fiber-reinforced polyethylene terephthalate, hot deformation temperature.

## Introduction

Polyethylene terephthalate (PET) is a familiar polymer with unique chemical composition,[1-2] molecular structure, typical chemical degradability, good comprehensive properties, and a lower price than most thermoplastics.[3-5] Adding glass fiber (GF) to PET can greatly improve the performance of PET.[6] In recent years, the development of GF-PET (PET reinforced by GF) as engineering plastics has been rapid, and it has been widely used in the fields of electronics, automobiles, and instrumentation. These fields require not only good mechanical and thermal properties but also good flame retardancy of materials. However, the limit oxygen index (LOI) of GF-PET is about 21%, making it a flammable material.[7-9] Therefore, improving the flame retardancy of GF-PET is of great significance. Scientific researchers have done substantial work and achieved certain accomplishments.[10-14]

In recent years, alkyl phosphonate metal salts have been effective flame retardants for polymer materials, with aluminum diethylphosphinate (ADP) being a typical representative.[15] There have been numerous research achievements in the field of polymer flame retardancy.[16-18] ADP was decomposed to form PO· and $PO_2$· free radicals, along with strong acids. The free radicals can inhibit combustion reactions, while the strong acids promote polymer dehydration and carbonization, thereby enhancing the composite's flame retardancy.[19-20] Boehmite (BM, γ-AlOOH), the main component of bauxite[21-22] and also known as soft bauxite,[23-24] is an important chemical raw material with a unique crystal structure and good thermal stability.[25-26] Due to the large amount of -OH groups on its surface,[27] BM tends to

†To whom correspondence should be addressed.
iverson25@126.com, ORCID 0000-0002-1394-3759

interact with foreign molecules, enabling the preparation of various composite functional materials.[28] The water vapor released during BM's thermal decomposition not only absorbs heat but also dilutes combustible gases generated by matrix decomposition. Simultaneously, the generated $Al_2O_3$ covers the material surface, promotes carbon formation, and enhances the flame retardancy of the polymer material.[29]

In this study, GF-PET, ADP/GF-PET, and BM/ADP/GF-PET composites were prepared, and the effects of BM and ADP on the flame retardancy, thermal properties, mechanical properties, and hot deformation temperature (HDT) of GF-PET were investigated. It was found that ADP could act as an effective flame retardant for GF-PET, while an appropriate amount of BM enhanced the flame retardancy, thermal properties, mechanical properties, and HDT of the ADP/GF-PET composite.

## Experimental

**Materials.** Polyethylene terephthalate (PET, CR-8816) was purchased from China Resources Chemical Materials Technology Co., LTD (Changzhou, China). Boehmite (BM, the effective substance content was ≧99%) was purchased from Shanghai Yanguo Chemical Co., LTD (Shanghai, China). Aluminum diethylphosphinate (ADP, the effective substance content was ≧99.9%) was purchased from Shouguanpur Chemical Co. LTD (Shouguang, China). Glass fiber (GF, 988A–2000) was purchased from Stonehenge Group Co. LTD (Jiaxin, China). Others (mixture of antidroppant, dispersant and antioxidant) were configured by the author's laboratory.

**Preparations of Samples.** When the amount of ADP was maintained below 12%, it was observed that the flame retardancy of the composite could not be achieved to meet the UL-94 3.0 mm V0 rating. Consequently, an ADP content of 12% was established as the base formulation. Formulations of the mixtures and abbreviations used for the respective composites were illustrated in Table 1. The PET, ADP and BM were premixed before being fed into the first zone of the extruder. All composites were prepared by using a twin screw extruder (SHJ-20 with the average screw diameter was 20 mm and the average L/D ratio was 40), with a temperature profile of 250-275 ℃ and a rotating speed of 150 rpm, and then the extruded strand was passed through a water bath and pelletized. The pellets were injected into ISO standard specimens by using an injection molding machine (HMT OENKEY, capacity 200 g). The processing conditions: injection molding temperature was 260-280 ℃, pressure was 65-75 bar, cooling time was 8s.

**Limit Oxygen Index (LOI) Measurement.** The limit oxygen index (LOI) was measured according to ISO 4589-2:2017 by an HC-2C oxygen index meter (Nanjing Shangyuan Analytical Instrument Co., LTD, China). The specimens used for the test had dimensions of 80 × 10 × 4 mm.

**Vertical Burning Test.** The underwriter laboratories 94 (UL-94) vertical burning test was performed using a vertical burning instrument (HVR-4type; Guangzhou Xinna Electronic Equipment Co., LTD, China), and the specimens for testing had dimensions of 128 × 12.8 × 3.0 mm and 128 × 12.8 × 2.0 mm.

**Cone Calorimeter Test.** Combustion behavior was studied using a cone calorimeter (UK Testing Technology Limited. UK) according to ISO 5660 at an external heat flux of 50 kW/m$^2$, and the specimens for testing had dimensions of 100 × 100 × 3.0 mm.

**Thermogravimetry Analysis.** Thermogravimetric analysis (TG) of the samples under air atmospheres was performed on a TAQ50 apparatus (TA Instruments Inc.USA). All the samples were heated from 35 ℃ to 750 ℃ at the rate of 10 ℃/min.

**Mechanical Properties Test.** The tensile and flexural tests were carried out by using a Universal Testing Machine (LLOYD LR100K, England) according to ISO standards 527-1 (speed of test 5 mm/min) and ISO standards 178 (three point bending, speed of test 2 mm/min) respectively. The notched Izod impact strengths were conducted following ISO standards 8256 (pendulum hammer 5.5J) with impact type test machine (ZBC-50, China). Five samples of each category were tested and their average values were reported.

**Hot Deformation Temperature (HDT) Test.** The hot deformation temperature of the materials was expressed by temperature

**Table 1. Formulations of the Mixtures and Abbreviations for Respective Composites**

| Sample | PET (%) | GF (%) | ADP (%) | BM (%) | Others (%) |
|---|---|---|---|---|---|
| GF-PET | 83 | 15 | - | - | 2 |
| ADP/GF-PET | 71 | 15 | 12 | - | 2 |
| 2-BM/ADP/GF-PET | 71 | 15 | 10 | 2 | 2 |
| 4-BM/ADP/GF-PET | 71 | 15 | 8 | 4 | 2 |
| 6-BM/ADP/GF-PET | 71 | 15 | 6 | 6 | 2 |

of deflection under load. The temperature of deflection under load test was carried out by using a thermal deformation temperature tester (HDT/V-3116, China) according to ASTM D648. The tests were made in quintuplicate and the results were reported as average.

## Results and Discussion

**Flame Retardancy of GF-PET, ADP/GF-PET, and BM/ADP/GF-PET Composites.** To investigate the effects of ADP and BM on the flammability properties of GF-PET composites, two combustion performance tests—the limit oxygen index and vertical combustion test—were conducted, with the results presented in Table 2.

According to Table 2, the LOI of GF-PET was 21.2%, burning up to the clamp in the UL-94 standard test and classifying it as a flammable material. When 12% ADP was added to GF-PET, the LOI of the ADP/GF-PET composite increased to 31.0%, achieving a UL-94 V0 rating at 3.0 mm thickness. This suggests that adding ADP can improve the flame retardancy of GF-PET because when ADP is thermally decomposed: (1) PO· and $PO_2$· free radicals are generated, which capture H· and -COOH· free radicals, inhibit chain reactions, and slow combustion kinetics;[17,30] (2) metaphosphoric acid forms poly metaphosphoric acid and a phosphate liquid film. This non-flammable film, combined with the strong acid's dehydration effect, isolates the material from air while promoting carbonization, thereby improving flame retardancy.[31]

Replacing part of ADP with BM resulted in the LOI and flame retardancy grade of the BM/ADP/GF-PET composite initially increasing and then decreasing with increasing BM substitution. This behavior may be attributed to two mechanisms during BM thermal decomposition: (1) generated water vapor absorbs heat (lowering surface temperature) while diluting combustible gases from matrix decomposition, enhancing gas-phase flame retardancy; (2) $Al_2O_3$ (from BM decomposition) integrates into the poly metaphosphoric acid liquid film (from ADP decomposition), improving film integrity and coverage to better isolate air, combustible gases, and heat,[32,33] thereby enhancing condensed-phase flame retardancy. When BM replaces a small amount of ADP (2% or 4% BM addition), the poly metaphosphoric acid liquid film (formed by thermal decomposition of residual ADP) sufficiently coats $Al_2O_3$ solids (from BM decomposition). Under these conditions, both gas-phase and condensed-phase flame retardancy effects in the BM/ADP/GF-PET composite are enhanced, leading to improved material flame retardancy. However, when BM excessively replaces ADP (6% BM addition), the poly metaphosphoric acid liquid film (from residual ADP decomposition) becomes insufficient to coat $Al_2O_3$ solids (produced by BM decomposition). This reduces the liquid film's compactness and coverage, leading to diminished condensed-phase flame retardancy in the BM/ADP/GF-PET composite and consequent deterioration of overall material flame retardancy.

When BM replacement increased from 4% to 6%, the condensed-phase flame retardancy reduction exceeded the gas-phase flame retardancy enhancement. This led to a net decrease in overall flame retardancy, thus demonstrating 4-BM/ADP/GF-PET's superior flame retardancy compared to 6-BM/ADP/GF-PET. The LOI of the 4-BM/ADP/GF-PET composite was 34.2%, representing a 3.2% increase over the ADP/GF-PET composite, with flame retardancy achieving a UL-94 V0 rating at 2.0 mm thickness.

**Combustion Behavior of GF-PET, ADP/GF-PET and BM/ADP/GF-PET Composites.** The cone calorimeter was usually used to evaluate the flammability characteristics and fire safety of polymer materials in a real fire condition. Heat release rate (HRR) and total heat rate (THR) curves of GF-PET, ADP/GF-PET and BM/ADP/GF-PET composites are presented in Figures 1 and 2. The corresponding combustion data, including time to ignition (TTI), peak of heat release rate (PHRR), total heat rate (THR), total smoke release (TSR), average effective

**Table 2. LOI Value and UL94 Rating of GF-PET, ADP/GF-PET and BM/ADP/GF-PET Composites**

| Sample | LOI (%) | UL94 | |
|---|---|---|---|
| | | 3.0 mm | 2.0 mm |
| GF-PET | 21.2 | — | — |
| ADP/GF-PET | 31.0 | V0 ($t_1$ = 4.8s, $t_2$ = 5.0s) | V1 ($t_1$ = 12.4s, $t_2$ = 17.1s) |
| 2-BM/ADP/GF-PET | 32.3 | V0 ($t_1$ = 2.7s, $t_2$ = 4.8s) | V0 ($t_1$ = 7.9s, $t_2$ = 12.2s) |
| 4-BM/ADP/GF-PET | 34.2 | V0 ($t_1$ = 1.8s, $t_2$ = 3.6s) | V0 ($t_1$ = 3.5s, $t_2$ = 4.7s) |
| 6-BM/ADP/GF-PET | 31.4 | V0 ($t_1$ = 3.7s, $t_2$ = 4.8s) | V0 ($t_1$ = 10.2s, $t_2$ = 14.6s) |

Note: "—" means burning to the fixture; "$t_1$" represents the average time of the first combustion; "$t_2$" is the average time for the second combustion.

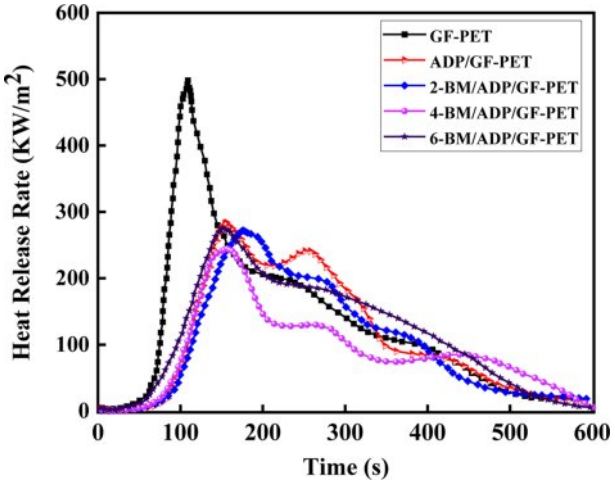


**Figure 1.** Heat release rate curves of GF-PET, ADP/GF-PET, and BM/ADP/GF-PET composites.

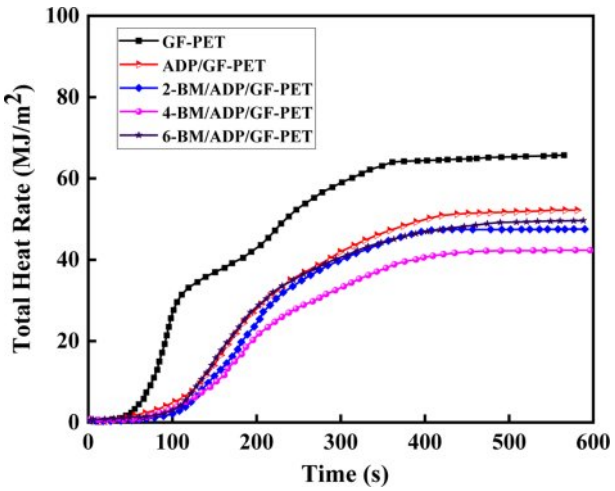


**Figure 2.** Total heat rate curves of GF-PET, ADP/GF-PET, and BM/ADP/GF-PET composites.

heat of combustion (AEHC) and fire performance index (FPI) are summarized in Table 3.

As can be seen from Figure 1, 2 and Table 3, when 12% ADP was added to GF-PET, the PHRR, AEHC, THR, and TSR of ADP/GF-PET composite were 284.1 $kW \cdot m^{-2}$, 18.6 $MJ \cdot kg^{-1}$, 52.1 $MJ \cdot m^{-2}$, and 1021.7 $m^2 \cdot m^{-2}$, which decreased by 43.0%, 4.1%, 20.7%, and 16.9% compared with GF-PET, respectively. The TTI and FPI of ADP/GF-PET composite were 47 $s \cdot m^2 \cdot kW^{-1}$ and 0.17 $s \cdot m^2 \cdot kW^{-1}$, which were 11.9% and 112.5% higher than that of GF-PET, respectively. This result shows that adding ADP to GF-PET prolongs the ignition time of composites and effectively inhibits combustion spread, burning intensity, and smoke emission in ADP/GF-PET composites. This behavior can be attributed to two mechanisms: (1) ADP decomposition generates $PO_2 \cdot$ and $PO \cdot$ radicals that terminate chain reactions by quenching H· and -COOH· radicals; (2) poly metaphosphoric acid (from ADP decomposition) crosslinks GF-PET decomposition products to form a compact char layer,[20,30] which restricts mass/heat transfer in combustion zones while improving flame retardancy.

Replacing part of ADP with BM resulted in the PHRR, THR, and TSR of the BM/ADP/GF-PET composite initially decreasing and then increasing with higher BM substitution, while the TTI and FPI first increased and then decreased. This trend may be attributed to two scenarios: (1) When BM replaces ADP in small quantities, it enhances the gas-phase flame retardancy of the BM/ADP/GF-PET composite. Simultaneously, the poly metaphosphoric acid liquid film (from residual ADP) sufficiently coats $Al_2O_3$ solids (via BM decomposition), enhancing coverage and compactness of the cover layer, thereby improving condensed-phase flame retardancy. So, the overall flame retardancy of BM/ADP/GF-PET was significantly enhanced. (2) When BM excessively replaces ADP, the condensed-phase flame retardancy of the BM/ADP/GF-PET composite deteriorates, with the extent of this degradation exceeding gas-phase enhancement. This imbalance ultimately reduces the composite's overall flame retardancy.

Unlike other indicators, the AEHC of the BM/ADP/GF-PET composite exhibited a gradual decrease with increasing BM replacement, demonstrating BM ability to enhance gas-phase flame retardancy. When 4% ADP was replaced by 4% BM, the 4-BM/ADP/GF-PET composite showed reductions in PHRR, AEHC, THR, and TSR by 13.9%, 16.7%, 18.8%, and 19.7%, respec-

**Table 3. Typical Parameters of GF-PET, ADP/GF-PET and BM/ADP/GF-PET Composites in the Cone Calorimetry Test**

| Sample | TTI (s) | PHRR ($kW \cdot m^{-2}$) | AEHC ($MJ \cdot kg^{-1}$) | THR ($MJ \cdot m^{-2}$) | TSR ($m^2 \cdot m^{-2}$) | FPI ($s \cdot m^2 \cdot kW^{-1}$) |
|---|---|---|---|---|---|---|
| GF-PET | 42 | 498.2 | 19.4 | 65.7 | 1230.1 | 0.08 |
| ADP/GF-PET | 47 | 284.1 | 18.6 | 52.1 | 1021.7 | 0.17 |
| 2-BM/ADP/GF-PET | 49 | 272.3 | 17.2 | 47.5 | 905.2 | 0.18 |
| 4-BM/ADP/GF-PET | 54 | 244.7 | 15.5 | 42.3 | 820.6 | 0.21 |
| 6-BM/ADP/GF-PET | 49 | 275.9 | 14.9 | 49.6 | 950.2 | 0.18 |

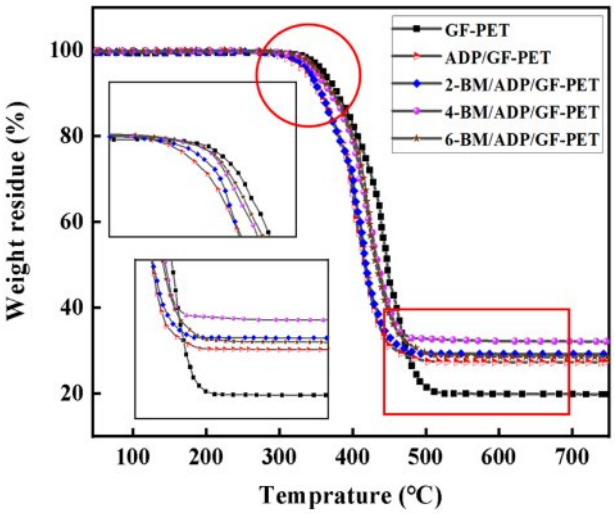


**Figure 3.** TG curves of GF-PET, ADP/GF-PET, and BM/ADP/GF-PET composites.

tively, while TTI and FPI increased by 14.9% and 23.5% compared to the ADP/GF-PET composite.

Thermal Degradation Behaviors of GF-PET, ADP/GF-PET, and BM/ADP/GF-PET Composites. The thermal degradation curves of GF-PET, ADP/GF-PET, and BM/ADP/GF-PET composites tested by TG in air are presented in Figure 3. The typical TG data in curves, including initial decomposition temperature ($T_{5\%}$), maximum decomposition temperature ($T_{max}$), maximum weight loss rate ($R_{max}$) and the char residue at 750 ℃ are summarized in Table 4.

When 12% ADP was added to GF-PET, the $T_{5\%}$ and $T_{max}$ of ADP/GF-PET composite were 336.2 ℃ and 392.1 ℃, respectively, which were lower than that of GF-PET, the $R_{max}$ was 21.2%·min$^{-1}$ and 13.5% less than that of GF-PET, the carbon residue at 750 ℃ was 27.3%, which increased by 37.9% compared with GF-PET. This occurred primarily because ADP's thermal decomposition temperature was lower than that of PET, causing ADP to decompose gradually prior to PET's thermal degradation. Consequently, the thermal degradation temperature of the ADP/GF-PET composite became lower than that of GF-PET. However, the poly metaphosphoric acid generated from ADP decomposition covered the material surface, insulating heat transfer, reducing the thermal decomposition rate, and promoting carbonization through dehydration. This resulted in the ADP/GF-PET composite exhibiting a lower maximum thermal weight loss rate and higher 750 ℃ residual char compared to GF-PET.

Replacing part of ADP with BM enhanced the $T_{5\%}$ and $T_{max}$ of the BM/ADP/GF-PET composite with increasing BM substitution. This improvement stemmed from water release during BM's thermal decomposition, where evaporation absorbed substantial heat, thereby elevating the composite's thermal decomposition temperature. Unlike $T_{5\%}$ and $T_{max}$, with increasing BM substitution amount, the $R_{max}$ of the BM/ADP/GF-PET composite first decreased and then increased, while the carbon residue at 750 ℃ of the BM/ADP/GF-PET composite first increased and then decreased. This phenomenon might be attributed to the fact that when BM small amount replaced ADP (2% or 4% BM addition), the liquid film of polymetaphosphoric acid generated by the remaining ADP was sufficient to fully cover the $Al_2O_3$ solid layer. The increased coverage area and compactness of the cover layer enhanced its thermal insulation capacity and ability to promote dehydration into carbon. Consequently, the decomposition rate of the material was reduced, while the high-temperature carbon residue content was increased. However, when excess BM replaces ADP (6% BM addition), the liquid film of poly metaphosphoric acid formed by thermal decomposition of the remaining ADP was insufficient to fully cover the $Al_2O_3$ solid layer. This resulted in reduced coverage area and compactness of the overall coating, diminished heat insulation capacity, weakened promotion of dehydration into carbon, and consequently decreased corresponding performance. In summary, the energy of heat insulation, oxygen isolation and promoting polymer into carbon of the cover layer formed by heating of 4-BM/ADP/GF-PET was better than that of 6-BM/ADP/GF-PET, so that the residual carbon amount of 4-BM/ADP/GF-PET at 750 ℃ was higher than that of 6-BM/ADP/GF-PET. When 4% ADP was replaced with 4% BM, the $T_{5\%}$

**Table 4. Typical Parameters of GF-PET, ADP/GF-PET, and BM/ADP/GF-PET Composites in the Thermogravimetric Analysis**

| Sample | $T_{5\%}$ (℃) | $T_{max}$ (℃) | $R_{max}$ (%·min$^{-1}$) | Char residue at 750 ℃ (%) |
|---|---|---|---|---|
| GF-PET | 362.1 | 421.5 | 24.5 | 19.8 |
| ADP/GF-PET | 336.2 | 392.1 | 21.2 | 27.3 |
| 2-BM/ADP/GF-PET | 341.5 | 398.2 | 20.1 | 29.2 |
| 4-BM/ADP/GF-PET | 347.8 | 406.5 | 18.4 | 32.1 |
| 6-BM/ADP/GF-PET | 352.4 | 412.7 | 20.6 | 28.5 |

**Table 5. Mechanical Properties of GF-PET, ADP/GF-PET, and BM/ADP/GF-PET Composites**

| Sample | Mechanical properties | | | |
|---|---|---|---|---|
| | Tensile strengths (MPa) | Flexural strengths (MPa) | Flexural modules (MPa) | Notched Izod impact strength ($kJ \cdot m^{-2}$) |
| GF-PET | 98.3 | 150.5 | 5248.6 | 7.4 |
| ADP/GF-PET | 85.2 | 132.3 | 5054.2 | 4.8 |
| 2-BM/ADP/GF-PET | 92.3 | 138.6 | 5120.7 | 5.5 |
| 4-BM/ADP/GF-PET | 101.5 | 148.4 | 5274.0 | 6.0 |
| 6-BM/ADP/GF-PET | 97.5 | 144.2 | 5296.3 | 5.3 |

and $T_{max}$ of the 4-BM/ADP/GF-PET composite increased by 3.5% and 3.7%, respectively, compared to the ADP/GF-PET composite. The $R_{max}$ of the 4-BM/ADP/GF-PET composite decreased by 13.2%, while its carbon residue at 750 ℃ increased by 17.6%.

Mechanical Properties of GF-PET, ADP/GF-PET, and BM/ADP/GF-PET Composites. The mechanical properties of GF-PET, ADP/GF-PET and BM/ADP/GF-PET were shown in Table 5. It could be observed that the tensile strengths, flexural strengths, flexural modules and notched Izod impact strength of ADP/GF-PET were decreased compare with GF-PET. The result was attributed the poor compatibility between ADP and PET. When a large amount of ADP was added to PET, agglomeration occurred, toincreased stress concentration points and decreased strength of the composite materials.

By replacing part of ADP with BM, as the BM substitution amount increased, the tensile strength, flexural strength, and notched Izod impact strength of BM/ADP/GF-PET initially increased and then decreased. The result might be attributed to the fact that BM, as a rigid material with a short rod structure, could transfer stress from the matrix to BM.[32] When BM replaced ADP in small amounts, the low content of BM had homogeneous dispersion and strong interfacial interactions in BM/ADP/GF-PET, thereby enhancing stress transfer from the matrix to BM and leading to higher strength. In contrast, when excess BM replaces ADP, BM tended to agglomerate and exhibited poor dispersion in BM/ADP/GF-PET.Unlike strengths, the flexural modules of BM/ADP/GF-PET increased with the increasing BM substitution amount, which was attributed to the restricted motion of polymer chains by BM and the resultant stiffening of the composites. The tensile strengths, flexural strength, flexural modules and notched Izod impact strength of 4-BM/ADP/GF-PET composite were 101.5 MPa, 148.4 MPa, 5274.0 MPa, and 6.0 $kJ \cdot m^{-2}$, respectively, which were 19.1%, 12.2%, 4.3%, and 25.0% higher than that of ADP/GF-PET composite.

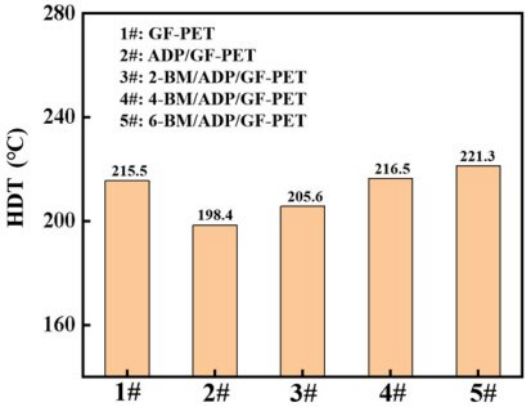


**Figure 4.** The HDT of GF-PET, ADP/GF-PET, and BM/ADP/GF-PET composites.

Hot Deformation Temperature (HDT) of GF-PET, ADP/GF-PET, and BM/ADP/GF-PET Composites. Figure 4 showed the deformation temperature of GF-PET, ADP/GF-PET and BM/ADP/GF-PET composites. Due to the poor compatibility between ADP and GF-PET, the HDT of ADP/GF-PET decreased relative to GF-PET. Like the flexural modules, the HDT of BM/ADP/GF-PET was increased with the increased of BM substitution amount. The result was attributed to the fact that BM, as a rigid material with a short-rod structure, restricted the motion of polymer chains, resulting in stiffer composites. This caused the deformation speed of the standard sample to decrease and the hot deformation temperature to increase under constant pressure. When the addition of BM was maintained below 4%, the enhancement in HDT of R-PET induced by BM was observed to be less significant than the reduction caused by ADP. Consequently, the HDT of sample 2-BM/ADP/GF-PET was demonstrated to be lower than that of sample GF-PET under the tested conditions. When the substitution of BM was 6%, the HDT of 6-BM/ADP/GF-PET composite reached 221.3 ℃, which was 22.9 ℃ higher than that of ADP/GF-PET.

## Conclusions

In conclusion, ADP was employed as a flame retardant for GF-PET, and a series of GF-PET composites were prepared. The results demonstrated that ADP effectively enhances GF-PET's flame retardancy. With 12% ADP addition, the ADP/GF-PET composite achieved an LOI of 31.0% and a UL-94 V0 rating at 3.0 mm thickness. The PHRR, AEHC, THR, and TSR of the ADP/GF-PET composite were lower than those of GF-PET, while the carbon residue at 750 ℃, TTI, and FPI were higher than those of GF-PET.

With the increase in BM substitution amount, the flame retardancy of the BM/ADP/GF-PET composite initially improved and then deteriorated. In combination with Tables 2, 3, and 4, the flame retardancy and thermal stability of composites containing 4% BM and 8% ADP (4-BM/ADP/GF-PET) were better than those with 12% ADP (ADP/GF-PET) alone, indicating that appropriate amounts of BM and ADP in GF-PET exhibited synergistic flame-retardant effects. Additionally, an appropriate amount of BM improved the mechanical properties and HDT of ADP/GF-PET.

Acknowledgment: We would like to thank A Project Supported by Scientific Research Fund of Hunan Provincial Education Department (NO.23C0611).

Conflict of Interest: The authors declare that there is no conflict of interest.

## References

1. Kim, S.; Hong, I. K.; Lee, S. Compatibilization of Linear PPS/PET Blends with SEBS Copolymers. *Polym. Korea* **2018**, 37, 405-410.
2. Lee, S.; Kang, S.; Kim, J. H. Electrical and Thermal Properties of PET/Polyetherimide/Multiwalled Carbon Nanotube Nanocomposites. *Polym. Korea* **2017**, 41, 287-294.
3. Mehdi, M.; Mahar, F. K.; Qureshi, U. A. Preparation of Colored Recycled Polyethylene Terephthalate Nanofibers From Waste Bottles: Physicochemical Studies. *Adv. Polym. Tech.* **2018**, 37, 2820-2827.
4. Louzada, N. D. L.; Malko, J. A. C.; Casagrande, M. D. Behavior of Clayey Soil Reinforced with Polyethylene Terephthalate. *J. Mater. Civil. Eng.* **2019**, 31,04019218.
5. Yin, Y.; Deng, P. Y.; Zhang, W. X.; Xing, Y. Effect of Enhanced Gamma-irradiation on the Compatibility of Polyethylene Terephthalate-based Basalt Fiber-reinforced Composites. *Adv. Polym. Tech.* **2018**, 37, 3376-3383.
6. Alqaflah, A. M.; Alotaibi, M. L.; Aldossery, J. N. Preparation and Characterization of Glass Fiber-reinforced Polyethylene Terephthalate/linear Low Density Polyethylene (GF-PET/LLDPE) Composites. *Polym. Adv. Tech.* **2018**, 29, 52-60.
7. Didane, N.; Giraud, S.; Devaux, E.; Lemort, G.; Capon, G. Thermal and Fire Resistance of Fibrous Materials Made by PET Containing Flame Retardant Agents. *Polym. Degrad. Stab.* **2012**, 97, 2545-2551.
8. Didane, N.; Giraud, S.; Devaux, E.; Lemort, G. Development of Fire Resistant PET Fibrous Structures Based on Phosphinate-POSS Blends. *Polym. Degrad. Stab.* **2012**, 97, 879-885.
9. Alongi, J.; Frache, A.; Gioffredi, E. Fire-retardant Poly(ethylene terephthalate) by Combination of Expandable Graphite and Layered Clays for Plastics and Textiles. *Fire. Mater.* **2011**, 35, 383-396.
10. Cai, Y.; Ke, H.; D.; Wei, Q.; Lin, J.; Yong, Z.; Lei, S.; Yuan, H.; Huang, F.; Gao, W. Effects of Nano-$SiO_2$ on Morphology, Thermal Energy Storage, Thermal Stability, and Combustion Properties of Electrospun Lauric Acid/pet Ultrafine Composite Fibers As Form-stable Phase Change Materials. *Appled. Energy* **2011**, 88, 2106-2112.
11. Zhang, X.; Wang, Q.; Liu, S.; Zhang, L.; Wang, G. Synthesis and Characterization of Fire-safety PET by Schiff Base With Nitro Group. *Eur. Polym. J.* **2021**, 145, 110230.
12. Yang, Y.; Niu, M.; Dai, J.; Bai, J.; Xue, B.; Song, Y.; Peng, Y. Flame-retarded Polyethylene Terephthalate with Carbon Microspheres/magnesium Hydroxide Compound Flame Retardant. *Fire. Mater.* **2018**, 42, 794-804.
13. Morgan, A. B.; Liu, W. D. Flammability of Thermoplastic Carbon Nanofiber Nanocomposites. *Fire. Mater.* **2011**, 35, 43-60.
14. Adner, D.; Helmy. M.; Otto, T.; schellenberg, J.; Schadewald, A. A Macromolecular Halogen-free Flame Retardant and Its Effect on the Properties of Thermoplastic Polyesters. *Fire. Mater.* **2019**, 43, 169-174.
15. Wang, Y.; Zhang, L.; Yang, Y.; Cai, X. Synergistic Fame Retardant Efects and Mechanisms of Aluminum Diethylphosphinate (AlPi) in Combination with Aluminum Trihydrate (ATH) in UPR. *J. Therm. Anal. Calorim.* **2016**, 125, 839-848.
16. Gu, L.; Qiu, J.; Sakai, E. Thermal Stability and Fre Behavior of Aluminum Diethylphosphinate-epoxy Resin Nanocomposites. *J. Mater. Sci. Mater. Electron.* **2016**, 28, 18-27.
17. Kaya, H.; Özdemir, E.; Kaynak, C.; Hacaloglu, J. Efects of Nanoparticles on Thermal Degradation of Polylactide/aluminium Diethylphosphinate Composites. *J. Anal. Appl. Pyrol.* **2016**, 118, 115-122.
18. Zhan, Z.; Xu, M.; Li, B. Synergistic Efects of Sepiolite on the Fame Retardant Properties and Thermal Degradation Behaviors of Polyamide 66/aluminum Diethylphosphinate Composites. *Polym. Degrad. Stab.* **2015**, 117, 66-74.
19. Ma, K.; Li, B.; Xu, M. J. Simultaneously Improving the Flame Retardancy and Mechanical Properties for Polyamide 6/aluminum Diethylphosphinate Composites by Incorporating of 1,3,5-triglycidyl Isocyanurate. *Polym. Adv. Tech.* **2018**, 29, 1068-1077.
20. Seefeldt, H.; Duemichen, E.; Braun, U. Flame Retardancy of

Glass Fber Reinforced High Temperature Polyamide by Use of Aluminum Diethylphosphinate: Thermal and Thermo-oxidative Efects. *Polym. Int*. **2013**, 62, 1608-1616.
21. Ceren, O.; Krzysztof, K.; Davidvander, B. Preparation and Properties of Polyamide-6-boehmite Nanocomposites. *Polymer* **2004**, 45, 5207-5214.
22. Laachachi, A.; Ferriol, M.; Cochez, M.; Cuesta, J. M. L.; Ruch, D. A Comparison of the Role of Boehmite (AlOOH) and Alumina ($Al_2O_3$) in the Thermal Stability and Flammability of Poly(methyl methacrylate). *Polym. Degrad. Stab.* **2009**, 94, 1373-1378.
23. Gatos, K. G.; Alcázar, J. G. M; Psarras, G. C.; Thomann, R.; Karger-Kocsis, J. Polyurethane Latex/water Dispersible Boehmite Alumina Nanocomposites: Thermal, Mechanical and Dielectrical Properties. *Compos. Sci. Technol.* **2007**, 67, 157-167.
24. Ceren, O.; Krzysztof, K.; Stephen, J. Preparation and Characterization of Titanate-modified Boehmite–polyamide-6 Nanocomposites. *Polymer* **2005**, 46, 6025-6034.
25. Ming, S. Y.; Mu, C. K.; Jyh, H. W. Functional Processing of PET Fabrics Using Boehmite/Silica/Thiazole Dye Hybrid Materials. *Fiber. Polym*. **2013**, 14, 1432-1439.
26. Camino, G; Maffezzoli, A.; Braglia, M.; Lazzaro, M. D.; Zammarano, M. Effect of Hydroxides and Hydroxycarbonate Structure on Fire Retardant Effectiveness and Mechanical Properties in Ethylene-vinyl Acetate Copolymer. *Polym. Degrad. Stab.* **2001**, 74, 457-464.
27. Pawlowski, K. H.; Schartel, B. Flame Retardancy Mechanisms of Aryl Phosphates in Combination with Boehmite in Bisphenol a Polycarbonate/acrylonitrilebutadiene-styrene Blends. *Polym. Degrad. Stab.* **2008**, 93, 657-667.
28. Li, M.; Sun, H. Y.; Liu, X. L. Preparation of Porous Boehmite Nanosolid and Its Composite Fluorescent Materials by a Novel Hydrothermal Hot-press Method. *Mater. Lett*. **2006**, 60, 2738-2742.
29. Marco, M.; Giovanni, C. Thermal and Combustion Behavior of Polyethersulfone-boehmite Nanocomposites. *Polym. Degrad. Stab.* **2013**, 98, 1838-1846.
30. Zhong, L.; Zhang, K. X.; Wang, X. Synergistic Efects and Fame-retardant Mechanism of Aluminum Diethyl Phosphinate in Combination with Melamine Polyphosphate and Aluminum Oxide in Epoxy Resin. *J. Therm. Anal. Calorim*. **2018**, 134, 1637-1646.
31. Li, X.; Fang S. G. Preparation and Property Analysis of Kaolin/melamine Cyanurate/aluminum Diethylphosphinate/recycled PET Composites. *J. Appl. Polym. Sci*. **2023**, 140, e53598.
32. Li, X. Infuence of Melamine Cyanurate and Boehmite on Flame Retardancy of PA6. *Iran. Polym. J.* **2022**, 31, 975-981.
33. Li, X.; Fang, S. G. Effect of Boehmite and Vermiculite on Flame Retardancy and Mechanical Properties of PET. *Polym. Korea* **2022**, 46, 463-469.